

Crystal Structure and Molecular Stereochemistry of Novel Polymeric $\text{Cu}_2(\text{DMP})_4(\text{DMSO})$ as a Platform for Phosphate Diester Binding

Massoud Rafizadeh,* Reza Tayebee,†,* Vahid Amani, and Mohammad Nasseh

Department of Chemistry, Tehran Teacher Training University, Tehran, Iran. *E-mail: rafizadeh@saba.tmu.ac.ir

†Department of Chemistry, Sabzevar Teacher Training University, Sabzevar, Iran. *E-mail: Rtayebee@sttu.ac.ir

Received December 17, 2004

Treatment of a solution of CuCl_2 in dimethyl phosphate (DMP) with DMSO under nitrogen atmosphere afforded a light blue fluorescence powder. Slow evaporation of H_2O -DMSO solution of this powder resulted in blue-sky crystals of a new polymeric $\text{Cu}(\text{II})$ complex, with a unit cell composed of $\text{Cu}_2(\text{DMP})_4(\text{DMSO})$, (**1**). The crystal and molecular structure of the complex acquired crystallographically. Compound (**1**) crystallizes in the monoclinic space group $\text{P}2_1/n$ with $a = 12.8920(11) \text{ \AA}$, $b = 13.1966(11) \text{ \AA}$, $c = 14.7926(13) \text{ \AA}$, $\alpha = 90^\circ$, $\beta = 98.943(2)^\circ$, $\gamma = 90^\circ$, $V = 2486.1(4) \text{ \AA}^3$, and $Z = 4$. A square pyramidal environment for the metal center was established by coordination of oxygen atoms of four bridging DMP ligands in the basal positions and binding a tri-centered oxygen atom of DMSO in the apical disposition of $\text{Cu}(\text{II})$. The sixth position was also affected by a weak interaction with the sulfur atom of another DMSO. The phosphorous atom in the bridging DMP was arranged in a deformed tetrahedron with (gg) conformation for methyl esters with C_{2v} symmetry.

Key Words : Dimethyl phosphate, Copper, Dimethyl sulfoxide, Synthesis, Structure

Introduction

One useful approach to the identification of metallo-enzymes which catalyze the hydrolysis of phosphate esters in biological molecules¹⁻⁴ is studying of similar model complexes which mimic the enzymatic role, structure, and reactivity of the active sites of these enzymes.⁵⁻⁸ Variation of ligands and changes in the coordination environment of these biological analogues have provided a valuable understanding of structure and function of important biomolecules. To achieve this goal, different polydentate ligands have been widely applied in the synthesis of discrete molecules with comparable structural and/or functional metal environments to those found in the enzymes.⁹⁻¹²

A wide range of metal complexes with a variety of central metal ions such as d-block transition metals^{5-10,12} and lanthanides^{11,12} are applied to investigate phosphate ester bonds. Different Mononuclear,¹³⁻¹⁵ binuclear,¹⁶⁻²⁷ trinuclear,^{28,29} tetranuclear³⁰⁻³³ and polymeric³⁴ heterometallic complexes bearing monodentate, chelating, and bridging phosphate moieties are being examined in order to find metal binding properties of such ligands and to elucidate the importance of these interactions in biological systems.³⁵

To the best of our knowledge, there are only a few papers on the complexation of DMP to the transition metals such as copper, nickel, and iron.³⁶ Now, we wish to introduce a novel polymeric copper complex, as a unique case for bridging coordination of DMP to $\text{Cu}(\text{II})$, within which an asymmetric binuclear constellation consisting of two copper ions are connected by four bridging DMP ligands and semi-bridging of one DMSO.

Experimental Section

Materials. Chemical reagents were obtained from commercial suppliers and used after further purification. Copper chloride was recrystallized and solvents were used as received or were distilled prior to use.

Instrumentation. Infrared spectra recorded using KBr disks on a Perkin-Elmer 8343 Spectrophotometer. ³¹P-nmr spectra recorded in D_2O on a Bruker-DRX 500-Avance Spectrometer. UV-vis spectra carried out on a Shimadzu-3100 Spectrophotometer. Solution spectra recorded in a 1cm quartz cell. Microanalyses performed on a GNBH-West Ger. elemental analyzer. Melting points obtained by using a Thermal 9100 Certain.

X-ray Structure Determination. The X-ray data were obtained on a diffractometer ($\text{Mo K}\alpha$, 0.71073 \AA radiation, graphite-monochromator) at $293(2) \text{ K}$. Data were collected to a maximum 2θ value of 58.0° and the structure was solved by automatic direct methods using SHELXS-97. The structure was refined by full-matrix least-square analysis on F^2 with SHELXL. Goodness-of-fit on F^2 was 1.098. The absorption correction was applied using the multi-scan technique by SADABS. The non-hydrogen atoms were refined anisotropically and all the hydrogen atoms were located from subsequent difference Fourier maps and refined with riding model to a final R indices (all data) of R_1 (0.0456), and WR_2 (0.0936). Final R indices for 2677 reflection with $[I > 2\sigma(I)]$ were $R_1 = 0.0408$, and $WR_2 = 0.0915$. Independent reflections and absorption coefficient were $6479[R(\text{int}) = 0.0217]$ and 2.127 mm^{-1} , respectively (Table 1).

ORTEP respective of $\text{Cu}_2(\text{DMP})_4(\text{DMSO})$ accompanying

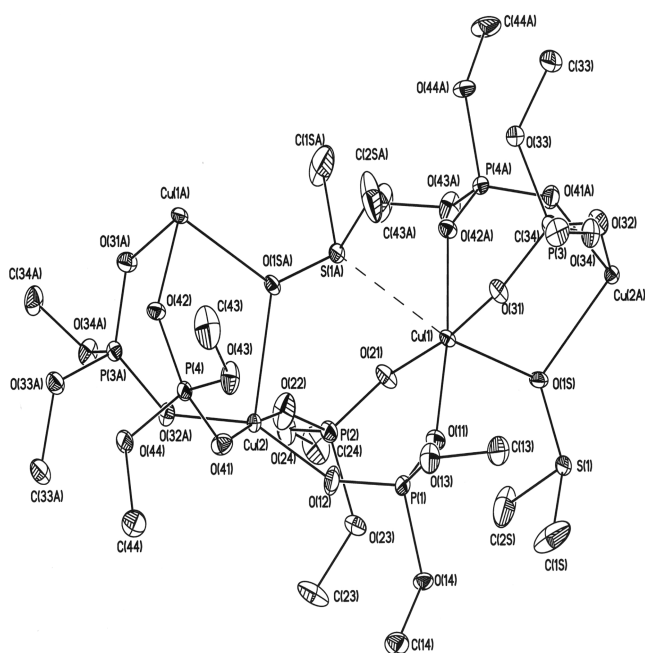


Figure 1. An ORTEP view of $\text{Cu}_2(\text{DMP})_4(\text{DMSO})$ with atomic labeling scheme. Selected bond distances (Å) and bond angles (deg.): Cu(1)-O(11) 1.9312(18), Cu(1)-O(42)#1 1.9341(18), Cu(1)-O(31) 1.9589(19), Cu(1)-O(21) 1.959(2), Cu(1)-O(1S) 2.353(2); O(11)-Cu(1)-O(42)#1 170.35(8), O(31)-Cu(1)-O(21) 171.75(9), O(11)-Cu(1)-O(1S) 98.22(8), O(21)-Cu(1)-O(1S) 95.06(8). Symmetry transformations used to generate equivalent atoms: #1 - $x + 1/2$, $y - 1/2$, $-z + 1/2$.

with the selected bond lengths and angles, and stereoview of the unit-cell packing of (1) are presented in Figures 1 and 2, respectively.

Synthesis and Characterization Data. $\text{Cu}_2(\text{DMP})_4(\text{DMSO})$ (1) was prepared by mixing of a solution of CuCl_2 (3.5 g) in dimethyl phosphate (14 mL) and DMSO (10 mL) under nitrogen atmosphere at 50 °C for 1 h. Light blue fluorescence powder (73% yield) was produced after slow evaporation of solvent. This product melts at 196 °C with found elemental analysis (%), C: 15.18; H: 3.86; P: 19.31. Slow evaporation of water-DMSO solution (1 : 1) of this product afforded blue-sky crystals of (1) after two weeks (yield 65%). Anal. Found for $\text{Cu}_2(\text{DMP})_4(\text{DMSO})$ (%), C: 16.86; H: 4.21; P: 17.5; S: 4.61. Calcd for (1)(%), C: 17; H: 4.2; P: 17.6; S: 4.5. These findings confirmed the empirical

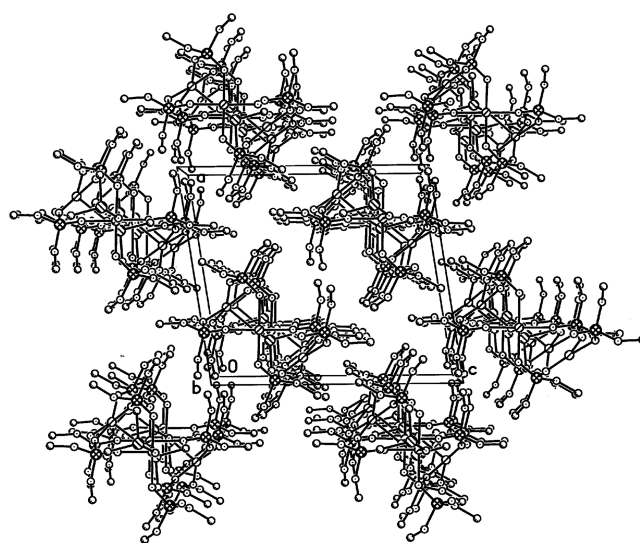


Figure 2. Stereoview of the unit-cell packing of $\text{Cu}_2(\text{DMP})_4(\text{DMSO})$.

formula of $\text{C}_{10}\text{H}_{30}\text{Cu}_2\text{P}_4\text{O}_{17}\text{S}$ (F.W., 705.36). ^{31}P -NMR revealed that all phosphorous atoms are identical.

Major IR bands (KBr; ν , cm^{-1}): 3000 w, 2959 w, 2859 w, 1461m, 1252 s sh, 1180 s, 1158 s, 1098 m, 1061 m, 1038 s, 849 s, 832 s, 779 s, 551 w, 521 s, 480 w.

Results and Discussion

Extensive quantum chemical studies have carried out on phosphodiester model compounds.⁴⁷ These investigations are employed to develop a comprehensive molecular force field for the phosphate group and to explore the conformational dependence of C-O-P-O-C skeletal vibrations. Within each charge group, the number and chemical nature of carbon substituent's also influence the phosphate geometry. These substituents affect the P-O bond distances and the O-P-O bond angles in the bridged bonds. Increase in the number of carbon substituent's shortens the bond length by 0.02 Å and enlarges the bond angle by 2-3° per substituent.

Dimethyl phosphate anion $(\text{CH}_3\text{-O})_2\text{-P}(\text{O})_2^-$ represents the smallest realistic model containing the C-O-P-O-C phosphodiester linkage of the nucleic acid backbone and phospholipids.³⁷ Common notations used in spectroscopy

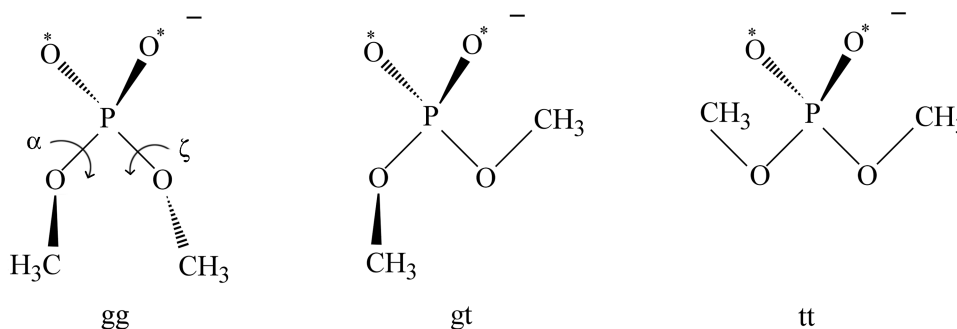


Figure 3. Gauche-gauche (gg), gauche-trans (gt) and trans-trans (tt) conformation of dimethyl phosphate anion.

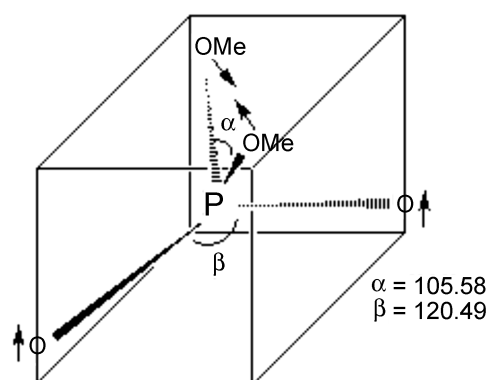


Figure 4. Simultaneous z-out and z-in distortions for DMP in $\text{Cu}_2(\text{DMP})_4(\text{DMSO})$.

suggest conformations with C-O-P-O(α, ζ) torsional angles of $\sim \pm 60$ (deg.) as gauche (g), and those of ~ 180 (deg.) as trans (t) for DMP. So the conformations are shown as gauche-gauche (gg), gauche-trans (gt), and trans-trans (tt), (Fig. 3). The energies of different conformers of DMP are

Table 1. Crystallographic data and data-collection parameters for the complex (**1**)

Chemical formula	$\text{Cu}_2(\text{DMP})_4(\text{DMSO})$
Empirical formula	$\text{C}_{10} \text{H}_{30} \text{Cu}_2 \text{P}_4 \text{O}_{17} \text{S}$
Formula weight	705.36
Temperature	120(2) K
Wavelength	0.71073 Å
Crystal system	Monoclinic
Space group	$\text{P} 2_1/n$
Unit cell dimensions	a = 12.8920(11) Å b = 13.1966(11) Å c = 14.7926(13) Å
α , deg	90°
β , deg	98.943(2)°
γ , deg	90°
Volume	2486.1(4) Å ³
Z	4
Density (calculated)	1.885 Mg/m ³
Absorption coefficient	2.127 mm ⁻¹
F(000)	1440
Crystal size	0.40 × 0.20 × 0.20 mm ³
Theta range for data collection	2.08 to 29.00°
Index ranges	-17 ≤ h ≤ 16, -11 ≤ k ≤ 18, -11 ≤ l ≤ 20
Reflections collected	13234
Independent reflections	6479 [R(int) = 0.0217]
Completeness to theta = 25.32°	98.0%
Max. and min transmission	0.9621 and 0.8251
Refinement method	Full-matrix least-squares on F ²
Data / restraints / parameters	6479 / 0 / 317
Goodness-of-fit on F2	1.098
Final R indices for 2677 refl. With [I > 2σ(I)]	R1 = 0.0408, wR2 = 0.0915
R indices (all data)	R1 = 0.0456, wR2 = 0.0936
Largest diff. peak and hole	1.027 and -1.016 e. Å ⁻³

calculated in order to determine the relative stability of the (gg), (gt), and (tt) conformations with a variety of theoretical models using HF3-21G(*) and 6-31G* and a large body of other works.^{38,39} These studies and also Monte-Carlo simulations of aqueous solvation of DMP^{40,41} have revealed that the (gg) conformer to be the most stable, followed by (gt) and (tt) conformations. The phosphate groups in $\text{Cu}_2(\text{DMP})_4(\text{DMSO})$ are arranged as a deformed tetrahedron. The average phosphate group has a 2-fold axis bisecting the two P-O bonds. Considering tetrahedral environment around the phosphorous, it is delineated that the dihedral angles are unequal. According to the data in Table 2, the angles of methoxy substituent's are unexpectedly smaller than the bridging oxygens. For example, the bond angle of MeO(13)-P(1)-O(14)Me moiety is 105.58°; whereas the bond angle of O(11)-P(1)-O(12) species is 120.49°. Subsequently, a simultaneous z-in and z-out distortions are suggested for DMP (Fig. 4). Presumably, there are no significant steric hindrances between methoxy substituent's in gauche-gauche dispositions.

Three distinct weak sharp bands of 2859, 2959, and 3000 cm^{-1} in the infrared spectral region belong to the stretching vibrations of methyl groups. Strong phosphate stretches at 1252 cm^{-1} . Five strong sharp bands at 1180, 1158, 1098, 1061, and 1038 cm^{-1} fit with the O-C stretches in P-O-C species and with the S-O stretches indicating the presence of DMSO. Band at 841 cm^{-1} corresponds to $\nu(\text{P-O})$ of P-O-C phosphate ester fragment. Several bands in the 480-550 cm^{-1} spectral region are assigned to the $\nu(\text{P-O-M})$ and $\nu(\text{S-O-M})$ stretching vibrations. However, position of $\nu(\text{S-O})$ in SOM(1)M(2) species bearing a three-centered oxygen, $\mu_3\text{-O}$, is not reported for DMSO. Therefore, it seems that $\nu(\text{S-O})$ stretching vibration overlaps with $\nu(\text{C-O})$ vibration of P-O-C species and $\nu(\text{M-O})$ vibration of S-O-M fragment, and determine the spectral pattern observed in the frequency region of $\nu(\text{P-O-M})$ stretching vibrations (480-600 cm^{-1}).⁴² Our experimental interpretations of the individual vibrational bands confirm the results of the previous findings on the infrared spectrum of solid NaDMP,⁴³ and other ab initio computational calculations such as normal coordinate analysis of DMP.⁴⁴

The aqueous solution electronic spectrum of (**1**) in which the central atom was surrounded in a square pyramidal environment, exhibits two strong $d \rightarrow d$ absorption maxima at 200-250 nm with a weak shoulder at 220 nm and a broad band at ~ 780 nm, which are in the typical range for $(dx^2-y^2)^1$ electronic ground-state of Cu(II) complexes with distorted square pyramidal geometry, commonly formed by DMP and DMSO ligands. These bands are in agreement with the $d_{z^2} \rightarrow d_{x^2-y^2}$ and $d_{xy} \rightarrow d_{x^2-y^2}$ electronic transitions.⁴⁵

Crystal Structure of $\text{Cu}_2(\text{DMP})_4(\text{DMSO})$. An x-ray structural analysis established that (**1**) consists of $\text{Cu}_2(\text{DMP})_4(\text{DMSO})$ fragments. ORTEP plot confirms two copper(II) ions are linked together *via* two O-P-O bridges and one oxygen atom of DMSO. The phosphate esters around each Cu stand nearly above the plane defined by four oxygen atoms of esters, and are directed to the DMSO

Table 2. Selected bond distances (Å) and bond angles (deg) in (1)

Cu(1)-O(11)	1.9312(18)
Cu(1)-O(42)#1	1.9341(18)
Cu(1)-O(31)	1.9589(19)
Cu(1)-O(21)	1.959(2)
Cu(1)-O(1S)	2.353(2)
Cu(1)-S(1) #2	3.1702(8)
P(1)-O(11)	1.485(2)
P(1)-O(12)	1.487(2)
P(1)-O(13)	1.577(2)
P(1)-O(14)	1.5900(19)
O(13)-C(13)	1.443(4)
O(14)-C(14)	1.442(3)
S(1)-O(1S)	1.5234(19)
S(1)-C(1S)	1.770(4)
S(1)-C(2S)	1.775(4)
O(11)-Cu(1)-O(42) #1	170.35(8)
O(11)-Cu(1)-O(31)	89.44(8)
O(42) #1-Cu(1)-O(31)	89.30(8)
O(11)-Cu(1)-O(21)	91.52(8)
O(42) #1-Cu(1)-O(21)	88.38(8)
O(31)-Cu(1)-O(21)	171.75(9)
O(11)-Cu(1)-O(1S)	98.22(8)
O(42) #1-Cu(1)-O(1S)	91.39(7)
O(31)-Cu(1)-O(1S)	92.91(8)
O(21)-Cu(1)-O(1S)	95.06(8)
O(11)-Cu(1)-S(1) #2	89.91(6)
O(42) #1-Cu(1)-S(1) #2	81.44(6)
O(31)-Cu(1)-S(1) #2	80.73(6)
O(21)-Cu(1)-S(1) #2	91.09(6)
O(1S)-Cu(1)-S(1) #2	170.43(5)
O(11)-P(1)-O(12)	120.49(12)
O(11)-P(1)-O(13)	111.44(12)
O(12)-P(1)-O(13)	105.16(12)
O(11)-P(1)-O(14)	103.76(11)
O(12)-P(1)-O(14)	109.55(12)
O(13)-P(1)-O(14)	105.58(11)
P(1)-O(11)-Cu(1)	149.09(13)
P(1)-O(12)-Cu(1)	146.75(14)
C(13)-O(13)-P(1)	118.92(19)
C(14)-O(14)-P(1)	118.57(18)
P(2)-O(21)-Cu(1)	128.04(12)
P(2)-O(22)-Cu(1)	151.83(15)
P(3)-O(31)-Cu(1)	130.93(12)
O(1S)-S(1)-C(1S)	107.11(15)
O(1S)-S(1)-C(2S)	105.85(15)
O(1S)-S(1)-C(2S)	98.5(2)
O(1S)-S(1)-Cu(1) #1	132.89(8)
C(1S)-S(1)-Cu(1) #1	98.38(13)
C(2S)-S(1)-Cu(1) #1	108.78(12)
S(1)-O(1S)-Cu(1)	132.90(11)
Cu(2) #1-O(1S)-Cu(1)	111.95(8)

Symmetry transformations used to generate equivalent atoms: #1- $x + 1/2, y - 1/2, -z + 1/2$. #2- $-x + 1/2, y + 1/2, -z + 1/2$

ligand. Therefore, according to the selected bond angles and bond lengths, each Cu(II) center occupies a distorted square

pyramidal (sp) geometry with the DMSO ligand in the apical and phosphate oxygen's in the basal dispositions. Consequently, the central atom as a "pivot atom" is displaced from the basal plane and the sulfur atom of the rear could not form the sixth bond completely (S(1)-Cu(1), 3.170 Å). Longer Cu(1)-O(1s) distance (2.353 Å), oxygen of DMSO in the apical position, than the other basal Cu-O distances is expectedly due to Jahn-Teller distortion in the d^9 Cu(II) center (Table 2). The Cu-O distances in the basal positions are typical of Cu(II) complexes for which the oxygen of either phosphate or phosphate diester is bound in an equatorial position.^{26,30} For comparison, the Cu-O distances of the apically coordinated phosphate moieties are *ca.* 0.2-0.3 Å longer.^{32,46}

The phosphorous atom environment in the ester adopts a significant distorted tetrahedral geometry. The distances of bridging phosphoryl oxygen's (*ca.* 1.485 Å) are shorter than the remaining P-O bonds of ester (*ca.* 1.590 Å), but are in typical range of copper-bound phosphate moieties.²⁶ Differences in bond angles of bridging and non-bridging O-P-O and R-O-P-O-R, respectively, fragments in (1) are more distinct than in similar compounds.²⁶

Binding and position of DMSO in (1) are also considerable. According to the x-ray measurements and data in Table 2, there is a weak interaction between S(1A) and Cu(1). The distance of S(1A)-Cu(1) is 3.170 Å, which confirms weak coordination of the sixth ligand to Cu(1). The oxygen of DMSO in (1) acts unexpectedly as a tri-centered nuclei. It is coordinated to the two copper centers and one sulfur atom. According to the bond lengths and angles around O(1s), its environment appears as a planar triangle. Large bond angle of Cu(1)-O(1s)-S(1), 132.9°, may belongs to the steric hindrances induced by methyl groups of DMSO with the Cu(1) environment. It is expected that O(1s) can be exchanged with analogous atoms and induces effective catalytic activity to the complex.

Since the phosphate group is an essential component in a variety of biological macromolecules,⁴⁴ synthesis and characterization of (1) provides further insights into the study of model compounds, that are important in several biological transformations. Investigations on the relevance of (1) to the phosphoryl transfer reactions and cleavage of phosphate esters are under consideration.

Crystallographic data for the structure reported here have been deposited with the Cambridge Crystallographic Data Center (Deposition No. CCDC-250661 (1)). These data can be obtained free of charge via <http://www.ccdc.cam.ac.uk/conts/retrieving.html> or from CCDC, 12 Union Road, Cambridge CB2 1EZ, UK, email: deposit@ccdc.cam.ac.uk.

Acknowledgements. The authors appreciate the financial support by Sabzevar and Tehran Teachers Training Universities.

References

1. Lipscomb, W. N.; Strater, N. *Chem. Rev.* 1996, 96, 2375.

2. Strater, N.; Lipscomb, W. N.; Klabunde, T.; Krebs, B. *Angew. Chem., Int. Ed. Engl.* **1996**, *35*, 2024.
 3. Gani, D.; Wilkie, J. *Struct. Bonding* **1997**, *89*, 133.
 4. Specific issue on RNA/DNA Cleavage: *Chem. Rev.* **1998**, *98*, 939.
 5. Kimura, E. *Prog. Inorg. Chem.* **1994**, *41*, 443.
 6. Kimura, E.; Koike, T.; Shionoya, M. *Struct. Bonding* **1997**, *89*, 1.
 7. Kimura, E.; Koike, T. *Adv. Inorg. Chem.* **1997**, *44*, 229.
 8. Kimura, E.; Kikuta, E. *Biol. Inorg. Chem.* **2001**, *5*, 139.
 9. Hegg, E. L.; Burstyn, J. N. *Coord. Chem. Rev.* **1998**, *173*, 133.
 10. Atkinson, I. M.; Lindoy, L. F. *Coord. Chem. Rev.* **2000**, *207*, 200.
 11. Komiyama, M. *J. Biochem.* **1995**, *118*, 665.
 12. Reichenbach-Klinke, R.; König, B. *J. Chem. Soc., Dalton Trans.* **2002**, 121.
 13. Weis, K.; Vahrenkamp, H. *Eur. J. Inorg. Chem.* **1998**, 271.
 14. Trosch, A.; Vahrenkamp, H. *Inorg. Chem.* **2001**, *40*, 271.
 15. Jurek, P. E.; Martell, A. E. *Inorg. Chem.* **1999**, *38*, 6003.
 16. Bazzicalupi, C.; Bencini, A.; Bianchi, A.; Fusi, V.; Giorgi, C.; Paoletti, P.; Valtancoli, B.; Zanchi, D. *Inorg. Chem.* **1997**, *36*, 2784.
 17. Jones, D. R.; Lindoy, L. F.; Sargeson, A. M.; Snow, M. R. *Inorg. Chem.* **1982**, *21*, 4155.
 18. Hikichi, S.; Tanaka, M.; Moro-oka, Y.; Kitajima, N. *J. Chem. Soc., Chem. Commun.* **1992**, 814.
 19. Wall, M.; Hynes, R. C.; Chin, J. *Angew. Chem., Int. Ed. Engl.* **1993**, *32*, 1633.
 20. Williams, N. H.; Lebus, A.-M.; Chin, J. *J. Am. Chem. Soc.* **1999**, *121*, 3341.
 21. Adams, H.; Bailey, N. A.; Fenton, D. A.; He, Q.-Y. *J. Chem. Soc., Dalton Trans.* **1995**, 697.
 22. Yan, S.; Pan, X.; Taylor, L. F.; Zhang, J. H.; O'Connor, C. J.; Britton, D.; Anderson, O. P.; Que, L. *Inorg. Chim. Acta* **1996**, *243*, 1.
 23. Kövari, E.; Krämer, R. *J. Am. Chem. Soc.* **1996**, *118*, 12704.
 24. Koike, T.; Inoue, M.; Kimura, E.; Shiro, M. *J. Am. Chem. Soc.* **1996**, *118*, 3091.
 25. He, C.; Gomez, V.; Spingler, B.; Lippard, S. *Inorg. Chem.* **2000**, *39*, 4188.
 26. Yamaguchi, K.; Akagi, F.; Fujinami, S.; Suzuki, M.; Shionoya, M.; Suzuki, S. *Chem. Commun.* **2001**, 375.
 27. Albehyl, S.; Averbuch-Pouchot, M. T.; Belle, C.; Krebs, B.; Pierre, J. L.; Saint-Aman, E.; Torelli, S. *Eur. J. Inorg. Chem.* **2001**, 1457.
 28. Kimura, E.; Aoki, S.; Koike, T.; Shiro, M. *J. Am. Chem. Soc.* **1997**, *119*, 3068.
 29. Spiccia, L.; Graham, B.; Hearn, M. T. W.; Lazarev, G.; Moubaraki, B.; Murray, K. S.; Tiekink, E. R. T. *J. Chem. Soc., Dalton Trans.* **1997**, 4089.
 30. Ye, B.-H.; Li, X.-Y.; Xue, F.; Mak, T. C. W. *Chem. Commun.* **1997**, 2407.
 31. Cargill Thompson, A. M. W.; Bardwell, D. A.; Jeffery, J. C.; Ward, M. D. *Inorg. Chim. Acta* **1998**, *267*, 239.
 32. Moubaraki, B.; Murray, K. S.; Ranford, J. D.; Wang, X.; Xu, Y. *Chem. Commun.* **1998**, 353.
 33. Paul, R. L.; Amoroso, A. J.; Jones, P. L.; Couchman, S. M.; Reeves, Z. R.; Rees, L. H.; Jeffery, J. C.; McCleverty, J. A.; Ward, M. D. *J. Chem. Soc., Dalton Trans.* **1999**, 1563.
 34. Angeloff, A.; Daran, J.-C.; Bernadou, J.; Meunier, B. *J. Organomet. Chem.* **2001**, *624*, 58.
 35. Yamami, M.; Furutachi, H.; Yokoyama, T.; Okawa, H. *Inorg. Chem.* **1998**, *37*, 6832.
 36. Fry, F. H.; Jensen, P.; Kepert, C. M.; Spiccia, L. *Inorg. Chem.* **2003**, *42*, 5637.
 37. Koldaivel, P.; Kanakaraju, R. *Int. J. Mol. Sci.* **2003**, *4*, 486.
 38. Liang, C.; Ewig, C. S.; Stouch, T. R.; Hagler, A. T. *J. Am. Chem. Soc.* **1993**, *115*, 1537.
 39. Landin, J.; Pascher, I.; Cremer, D. *J. Phys. Chem.* **1995**, *99*, 4471.
 40. Alagona, G.; Ghio, C.; Kollman, P. *J. Am. Chem. Soc.* **1983**, *105*, 5226.
 41. Jayaram, B.; Ravishanker, G.; Beveridge, D. L. *J. Phys. Chem.* **1988**, *92*, 1032.
 42. Nakamoto, K. In *Infrared and Raman Spectra of Inorganic and Coordination Compounds*, 5 ed.; John Wiley: New York, 1997; p 102.
 43. Fry, F. H.; Jensen, P.; Kepert, C. M.; Spiccia, L. *Inorg. Chem.* **2003**, *42*, 5637.
 44. Florian, J.; Baumruk, V.; Strajbl, M.; Bednarova, L.; Stepanek, J. *J. Phys. Chem.* **1996**, *100*, 1559.
 45. Graham, B.; Fallon, G. D.; Hearn, M. T. W.; Spiccia, L.; Moubaraki, B.; Murray, K. S. *J. Chem. Soc., Dalton Trans.* **2002**, 1226.
 46. Ott, R.; Kramer, R. *Angew. Chem., Int. Ed.* **1998**, *37*, 1957.
 47. Schneider, B.; Kabelac, M.; Hobza, P. *J. Am. Chem. Soc.* **1996**, *118*, 12207.
-